Entanglement Assisted Probe of the Non-Markovian to Markovian Transition in Open Quantum System Dynamics

Chandrashekhar Gaikwad,[1,*] Daria Kowsari,[1,2,3,*] Carson Brame,[1] Xingrui Song,[1] Haimeng Zhang,[2,4] Martina Esposito,[5] Arpit Ranadive,[6] Giulio Cappelli,[6] Nicolas Roch,[6] Eli M. Levenson-Falk,[2,3,4] and Kater W. Murch[1,†]

[1]*Department of Physics, Washington University, St. Louis, Missouri 63130, USA*
[2]*Center for Quantum Information Science and Technology, University of Southern California, Los Angeles, California 90089, USA*
[3]*Department of Physics & Astronomy, University of Southern California, Los Angeles, California 90089, USA*
[4]*Ming Hsieh Department of Electrical & Computer Engineering, University of Southern California, Los Angeles, California 90089, USA*
[5]*CNR-SPIN Complesso di Monte S. Angelo, via Cintia, Napoli 80126, Italy*
[6]*Université Grenoble Alpes, CNRS, Grenoble INP, Institut Néel, 38000 Grenoble, France*

(Received 24 January 2024; accepted 16 April 2024; published 13 May 2024)

We utilize a superconducting qubit processor to experimentally probe non-Markovian dynamics of an entangled qubit pair. We prepare an entangled state between two qubits and monitor the evolution of entanglement over time as one of the qubits interacts with a small quantum environment consisting of an auxiliary transmon qubit coupled to its readout cavity. We observe the collapse and revival of the entanglement as a signature of quantum memory effects in the environment. We then engineer the non-Markovianity of the environment by populating its readout cavity with thermal photons to show a transition from non-Markovian to Markovian dynamics, ultimately reaching a regime where the quantum Zeno effect creates a decoherence-free subspace that effectively stabilizes the entanglement between the qubits.

DOI: 10.1103/PhysRevLett.132.200401

Decoherence is a ubiquitous challenge in quantum technologies. At a microscopic level, decoherence arises from the entanglement of a quantum system with degrees of freedom in its environment. Without access to these degrees of freedom, information about the quantum state is lost [1,2]. The monotonic reduction in a quantum state's coherence is typically described by the well-known Gorini-Kossakowski-Sudarshan-Lindblad (GKSL) master equation [3,4] for the system's density operator ρ. In particular, the GKSL master equation is valid under the Born-Markov set of approximations, which assume both weak coupling to the environment, and that the environment is Markovian, i.e., memoryless [5]. This mathematically amenable description is surprisingly effective in describing a broad range of quantum dynamics. Moreover, in the Markovian regime, dissipation engineering by an intentional introduction of Markovian dissipation has been employed as a powerful method of quantum control; with applications including error correction [6–8], state preparation [9,10], state stabilization [11,12], and quantum simulation [13]. Naturally, however, there is another paradigm of decoherence known as the non-Markovian regime, where quantum memory effects induced by large system-environment correlations thwart a Markovian description. In this regime, the dynamics of the system is governed by the generalized Nakajima-Zwanzig master equation [14,15] which incorporates the memory effects of the environment.

Non-Markovian dynamics have the potential to enable novel applications stemming from memory effects in the environment, such as new approaches towards fault-tolerant quantum computation [16–18], quantum control [19], fidelity improvement in the implementation of the teleportation algorithms [20], and coherence preservation [21]. The non-Markovianity of an open quantum system can be measured using two common methods [22]. The most prominent measure is known as the trace distance method proposed by Breuer *et al.* [23], which relies on the fact that any completely positive trace-preserving (CPTP) quantum map between two-time steps will only result in a decrease of the distinguishability between two quantum states, hence any increase in the distance between states is associated with memory effects [24]. Later, an entanglement measure was introduced by Rivas *et al.* [25], where one probes quantum memory effects by allowing part of an entangled pair to interact with an environment. Again, a CPTP map will only decrease the degree of entanglement and an increase in entanglement during the system evolution is a signature of quantum memory effects. Both methods [26] have been employed to observe signatures of non-Markovianity, notably in nitrogen-vacancy centers [27–30], photonic systems [31–35], nuclear magnetic resonance [35–37], trapped ions [38], and on superconducting processors [39].

In this Letter, we harness the entanglement between two superconducting qubits as a probe of quantum memory

effects. We initialize the qubits in a Bell state and study the qubits' concurrence [40] over time as one of the qubits interacts with a small quantum environment consisting of a third qubit dispersively coupled to a microwave resonator. We observe collapse and then revival of the qubits' concurrence as a clear signature of the non-Markovian nature of the environment as the qubit becomes entangled and then disentangled with the environment. The non-Markovianity of the environment is then tuned by introducing Lindblad dephasing on the environment [41]. This allows us to investigate a transition away from non-Markovian dynamics to a regime where the GKSL master equation describes the dynamics. Since the GKSL master equation requires a Markovian approximation, we refer to this regime as the Markovian regime. In this Markovian regime, we further increase the dissipation on the environment, ultimately reaching a regime where the quantum Zeno effect pins the environment state, thereby preserving the qubits' entanglement.

Figure 1(a) displays the basic setup of the experiment, with the system Hamiltonian given in [42]. The experiment comprises a three-qubit processor with individual readout resonators dispersively coupled to each qubit and nearest-neighbor qubits sharing a resonator mediated coupling. The readout resonators allow us to perform individual state readouts of the three qubits by probing the associated microwave resonators with a microwave drive. We first focus on a subportion of the processor with two qubits denoted as the "Qubit" and the "Ancilla." The Qubit is frequency tunable via a superconducting quantum interference device (SQUID) loop and the Ancilla is fixed-frequency, both designed to be in the transmon regime [51]. In order to minimize the decoherence effects from flux noise, we operate the Qubit at its flux sweet spot and introduce coupling to the Ancilla via parametric modulation [52]. To this end, we apply an ac radio frequency drive on the Qubit fast flux line at roughly half the detuning between the Qubit and Ancilla [Fig. 1(b)]. We identify the resonance condition between the Qubit and Ancilla by initializing the qubit in its excited state and then applying the parametric modulation for a variable duration. Figure 1(c) shows the time evolution of the Ancilla $\langle \sigma_z \rangle \equiv Z_A$ near the parametric resonance. We observe a clear chevron profile with detuning from which we extract a parametric coupling rate of $\Omega_{Q,A}/2\pi = 0.477$ MHz.

We utilize this parametric coupling to produce a Bell state between the Qubit and Ancilla, as depicted in Fig. 2(a). After applying a π rotation to the Qubit, we activate the parametric coupling for 530 ns, corresponding to a $\sqrt{i\mathrm{SWAP}}$ gate, in principle, leaving the Qubit and Ancilla in a state, $(1/\sqrt{2})(|10\rangle + e^{i\phi}|01\rangle)$ [53]. We utilize quantum state tomography of the Qubit and Ancilla to characterize the resulting entangled state. For this, we measure nine Pauli expectation value pairs, $\{\langle \Sigma_Q \Sigma_A \rangle\}$, with $\Sigma_{Q,A} \in \{X, Y, Z\}$ by simultaneously measuring the

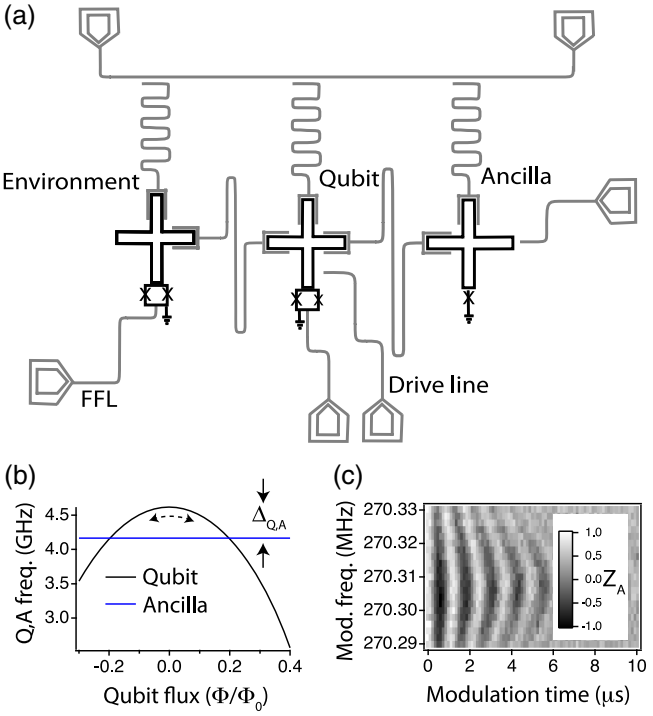

FIG. 1. Experiment setup. (a) Sketch of the experiment which includes three qubits respectively labeled "Environment," "Qubit," and "Ancilla." The qubits share resonators that mediate nearest-neighbor coupling. Each qubit is coupled to a readout resonator, which can be probed by a common feedline. The Environment and Qubit are frequency tunable via on-chip fast flux lines (FFLs). (b) The respective frequencies of the Qubit and Ancilla; resonant coupling between the qubits is achieved by applying a parametric modulation of the Qubit at roughly $\Delta_{Q,A}/2$. (c) When the Qubit is prepared in its excited state, parametric resonance can be observed by examining the Ancilla excitation versus modulation frequency.

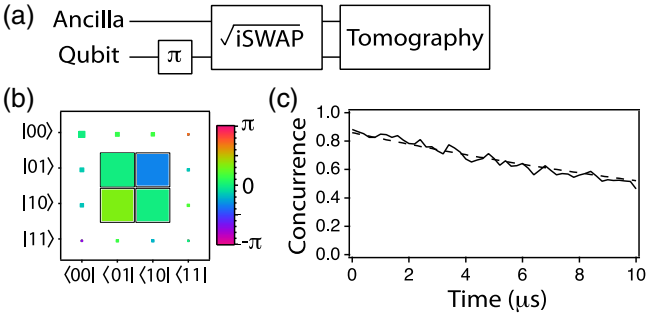

FIG. 2. Qubit-Ancilla entanglement. (a) We prepare an entangled state by initializing the Qubit in the excited state, and then applying a $\sqrt{i\mathrm{SWAP}}$ gate via parametric modulation. (b) Quantum state tomography allows us to reconstruct the Qubit-Ancilla density operator, yielding an entangled state of the form $(1/\sqrt{2})(|10\rangle + e^{i\phi}|01\rangle)$. (c) The measured Qubit-Ancilla concurrence versus time (solid line); we observe a monotonic decrease in the entanglement over time consistent with the single-qubit dephasing rates (dashed line).

state of both the Qubit and Ancilla [54]. The average readout fidelities of the Qubit and Ancilla are respectively 0.97 and 0.96. As discussed in the Supplemental Material, we use a maximum likelihood estimation method [55] to determine the components of the Qubit-Ancilla density matrix, displayed in Fig. 2(b). We observe a Bell state fidelity of 0.91, corresponding to a concurrence of 0.89.

With the Qubit and Ancilla entangled, we now study the evolution of the entanglement over time as the system sits idle. We display the Qubit-Ancilla concurrence versus time in Fig. 2(c). The concurrence slowly decreases over a timescale consistent with the respective individual dephasing times of the Qubit ($T_2^{*(Q)} = 39$ μs) and Ancilla ($T_2^{*(A)} = 41$ μs), e.g., $\mathcal{C} \propto \exp(-t/T_2^{*(Q)} - t/T_2^{*(A)})$, as given by the dashed line in Fig. 2(c).

We now turn to studying the interaction of the Qubit-Ancilla subspace with the Environment. As displayed in Fig. 3(a), after preparing the Qubit-Ancilla in an initial Bell state, we introduce a parametric coupling between the Qubit and Environment. In this case, we apply flux modulation simultaneously to both the Qubit and Environment [Fig. 3(b)] bringing the two into parametric resonance. Both Qubit and Environment are modulated at approximately one-quarter of their detuning ($\Delta_{Q,E}/4 = 2\pi \times 175$ rad/μs), which introduces a resonant transverse coupling between the Qubit-Environment pair at a rate of $\Omega_{Q,E} = 2\pi \times 0.473$ rad/μs, limited by the resonator-mediated coupling between the pair. After applying the parametric coupling between Qubit and Environment, we perform quantum state tomography on the Qubit-Ancilla subsystem to determine the remaining concurrence.

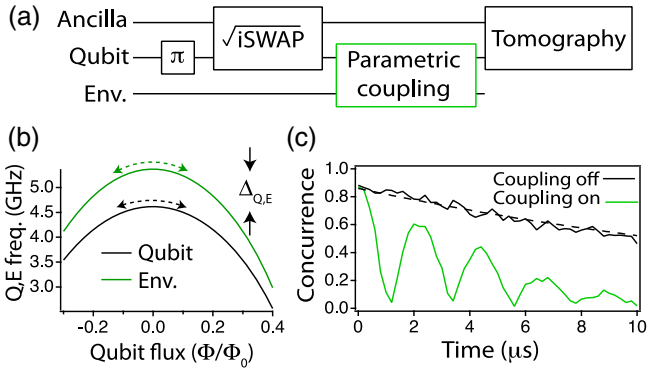

FIG. 3. Concurrence revival due to non-Markovianity. (a) We prepare an entangled state between the Qubit and Ancilla, then we apply a parametric coupling between the Qubit and Environment, finally, we perform a set of tomography pulses to reconstruct the density matrix of the Qubit-Ancilla subspace. The concurrence evolution is realized by varying the length of the Qubit-Environment parametric coupling pulses. (b) The respective frequencies of Qubit and Environment showing the Qubit-Environment detuning. (c) Concurrence evolution as a function of the Qubit-Environment parametric coupling pulse length (green). The black curve shows the concurrence evolution when the parametric coupling is turned off.

Figure 3(c) displays the evolution of the concurrence when the interaction between the Qubit and Environment is introduced. In comparison to the monotonic decrease in entanglement observed previously (black curve), we now note a rapid decrease in entanglement, with clear revivals at later times (green curve). The initial decrease is expected from the principle of monogamy of entanglement [56]. Since the Qubit-Ancilla system is in a maximally entangled state, the entanglement between the Qubit-Environment introduced by the parametric coupling must cause the Qubit-Ancilla entanglement to decrease. The revival of entanglement occurs as the Qubit-Environment coupling continues and the Environment state is swapped back into the Qubit. This revival of entanglement is a clear indicator of non-Markovianity, indicating that the environment has quantum coherent memory. This is indeed expected since the environment is itself a simple two-level system. The non-Markovianity of the system can be calculated as [25]

$$\mathcal{N} = \int_{t_0}^{t_f} dt \left| \frac{d\mathcal{C}[\rho_{Q,A}(t)]}{dt} \right| - \Delta\mathcal{C}, \tag{1}$$

where $\mathcal{C}[\cdots]$ denotes the concurrence measure, $\Delta\mathcal{C}$ is the difference in the concurrence at the initial and final steps of the evolution, and $\rho_{Q,A}$ represents the Qubit-Ancilla density matrix. To elaborate, we look at the time derivative of the concurrence over the entire time evolution of the system $\in [t_0 = 0\ \mu s, t_f = 10\ \mu s]$ at discrete time steps. It is clear from Eq. (1) that the positive slope of the concurrence contributes to the non-Markovianity measure. By applying Eq. (1) to the data in Fig. 3(c), we achieve a non-Markovianity of $\mathcal{N} = 1.4$.

With a clear demonstration of non-Markovian dynamics, we now study how this measure changes as the memory of the Environment is tuned. We achieve this by expanding the size of the Environment to include the quantum states of light that occupy the microwave resonator that is dispersively coupled to the Environment. So far, we have considered this resonator to remain in the vacuum state, which does not affect the Environment's memory. Now, we introduce pseudothermal photons into this resonator via a noisy microwave drive as indicated in Fig. 4(a). The interaction between the Environment and its resonator is captured by the simple dispersive coupling Hamiltonian, $H_{int} = \chi a^\dagger a \sigma_z^E$, where $\chi/2\pi = 200$ kHz is the dispersive coupling rate, $a^\dagger a$ is the resonator photon number, and σ_z^E is the Pauli operator that acts on the Environment in the energy basis. This interaction can be viewed as either an Environment-state-dependent frequency shift on the resonator frequency, whereby photons carry away information about the state of the Environment, or as an ac-Stark shift of the qubit frequency, whereby the fluctuating intraresonator photon number dephases the qubit [57].

The noisy drive on the cavity is chosen to have a bandwidth (1.8 MHz) that exceeds χ, ensuring a uniform

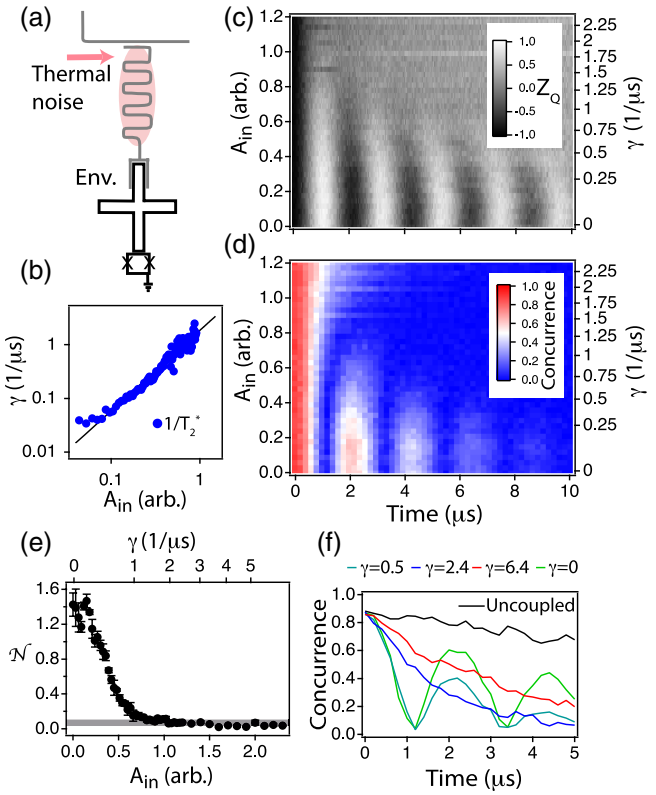

FIG. 4. Non-Markovian to Markovian transition. (a) By driving the Environment's readout resonator with pseudothermal noise of amplitude A_{in} we tune the Environment's memory. (b) This memory is quantified through Ramsey measurements on the Environment to determine the dephasing rate γ versus A_{in}. (c) For each value of A_{in} we calibrate the frequency of the parametric drive between the Qubit and Environment by studying Z_Q versus time and maximizing the population transfer [42]. (d) The Qubit-Ancilla concurrence versus time for different Environment dephasing rates. The transition to monotonic behavior indicates the transition from non-Markovian to Markovian dynamics. (e) The non-Markovian measure (1) quantified across the transition. The error bars indicate the standard error of the mean from three independent experimental trials. The gray bar indicates the measure applied to the case where the Environment is decoupled and characterizes the background of the measure. (f) The concurrence versus time for a few specific dephasing rates (expressed in units of μs^{-1}).

drive independent of the Environment state. Furthermore, this drive is set to have a correlation time (90 ns) much shorter than any other timescale of the dynamics, allowing us to treat its dephasing effect as Markovian. We calibrate the dephasing via direct Ramsey measurements on the Environment. This establishes a relationship between the dephasing rate and the noise amplitude (A_{in}) as shown in Fig. 4(b). We find an empirical relationship for the Environment dephasing $\gamma = 1.84\ (\mu s)^{-1} A_{\mathrm{in}}^{1.5}$, as given by the black line in Fig. 4(b).

The introduction of the thermal photons into the Environment causes slight shifts in the parametric coupling between the Qubit and the Environment. As such, we calibrate the parametric coupling between the Qubit and Environment for each value of A_{in}. Figure 4(c) shows the resulting parametric coupling between the Qubit and Environment when the Qubit is initialized in the excited state and the parametric coupling is activated for a variable duration of time. By increasing the dephasing of the Environment, we observe diminished population transfer contrast between the Qubit and the Environment.

Next, we investigate the time evolution of the Qubit-Ancilla concurrence for different values of the Environment dephasing. Increasing the Environment dephasing induces a transition from non-Markovian to Markovian dynamics as displayed in Fig. 4(d). We quantify the transition away from non-Markovian dynamics via the measure [Eq. (1)] as displayed in Fig. 4(e); as the dephasing of the Environment is increased beyond $\gamma \simeq 1\ (\mu s)^{-1}$, $\mathcal{N}$ becomes consistent with zero. However, the dynamics are not immediately Markovian, which we define by the applicability of the GKSL master equation to the Qubit-Ancilla subsystem. As we study in [42], the GKSL master equation yields exponentially decaying dynamics of the concurrence. This matches well the measured dynamics for $\gamma \gtrsim 3\ (\mu s)^{-1}$, but fails to capture the dynamics for smaller values of γ. As such, the transition between these two regions, as defined, is not abrupt.

In Fig. 4(f) we display the concurrence versus time for a few selected values of γ. We note two important trends; first, in the non-Markovian regime, increasing dephasing accelerates the decay envelope of the concurrence (compare $\gamma = 0$ and $\gamma = 0.5$), and second, in the Markovian regime, further increasing dephasing slows the decay of the concurrence ($\gamma = 2.4$ and $\gamma = 6.4$). This can be understood within the context of the quantum Zeno effect [58–65]. The thermal photons perform measurement (at rate γ) of the Environment, which slows the coupling induced by the parametric drive. In Fig. 5, we explore in detail how the dephasing of the Environment affects the Qubit-Ancilla entanglement. Figure 5(a) displays the concurrence versus time for several values of the dephasing in the Markovian regime. For increasing measurement on the Environment, we see that the decay of concurrence is slowed, approaching the limiting case where the Qubit is completely uncoupled from the Environment. We characterize the exponential decay of the concurrence with a rate Γ_c, and display this rate versus Environment dephasing in Fig. 5(b) in both the non-Markovian and Markovian regimes; the transition between these two regimes coincides with the onset of Zeno stabilization of the entanglement. Under the standard analysis of the Zeno effect [63,66], we expect $\Gamma_c = \Omega_{\mathrm{Q,E}}^2/4\gamma + \Gamma_0$. Here $\Gamma_0 = 1/T_2^{*Q} + 1/T_2^{*A}$ is the decay rate of the concurrence when the Environment is decoupled. We observe close agreement with this expected scaling (red curve). This demonstrates a new approach to

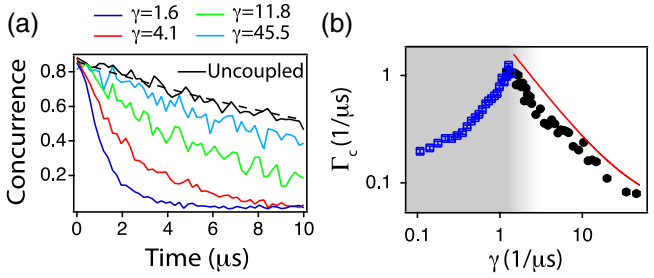

FIG. 5. Quantum Zeno stabilization of entanglement. (a) Qubit-Ancilla concurrence versus time for different Environment dephasing rates; as the dephasing increases, the entanglement decay approaches the uncoupled case consistent with the Qubit and Ancilla's individual dephasing rates. (b) The exponential decay rate of the concurrence (Γ_c) versus Environment dephasing rate. The gray region indicates the non-Markovian regime, where we determine Γ_c by fitting the overall (nonmonotonic) decay envelope of the concurrence. In the Markovian regime, we observe that the Zeno effect suppresses the concurrence decay induced by the environment, in agreement with the expected scaling (red line).

preserving quantum entanglement via Zeno-enabled pinning of environment states.

In conclusion, we have quantified the transition from non-Markovian dynamics to Zeno dynamics with an entanglement-assisted probe. Importantly, the probe is sensitive to the quantum memory of the environment; a classical environment that stores populations will not result in the revival of concurrence for the entangled probe. This approach can have utility in the test of the quantum nature of decoherence channels (e.g., in testing models of quantum gravity [67]). Moreover, by introducing controllable dissipation on the environment we observe stabilization of the Qubit-Ancilla subsystem, highlighting how dissipation forms a powerful tool for quantum subspace engineering [13].

The authors are thankful for the useful discussions with Daniel Lidar, Kade Head-Marsden, Patrick Harrington, Weijian Chen, Kaiwen Zheng, Maryam Abbasi, Serra Erdamar, and Archana Kamal. This research was supported by NSF Grants No. PHY-1752844 (CAREER) and No. OMA-1936388, the Air Force Office of Scientific Research (AFOSR) Multidisciplinary University Research Initiative (MURI) Award on Programmable systems with non-Hermitian quantum dynamics (Grant No. FA9550-21-1- 0202), the John Templeton Foundation, Grant No. 61835, ONR Grants No. N00014-21-1-2630 and No. N00014-21-1-2688 (YIP), Research Corp. Grant No. 27550 (Cottrell), European Union's FET Open AVaQus Grant No. 899561 and Marie Sklodowska-Curie Grant No. MSCA-IF-835791. Devices were fabricated and provided by the Superconducting Qubits at Lincoln Laboratory (SQUILL) Foundry at MIT Lincoln Laboratory, with funding from the Laboratory for Physical Sciences (LPS) Qubit Collaboratory.

*These authors contributed equally to this letter.
†murch@physics.wustl.edu

[1] Wojciech Hubert Zurek, Decoherence, einselection, and the quantum origins of the classical, Rev. Mod. Phys. **75**, 715 (2003).
[2] Ph. Jacquod and C. Petitjean, Decoherence, entanglement and irreversibility in quantum dynamical systems with few degrees of freedom, Adv. Phys. **58**, 67 (2009).
[3] G. Lindblad, On the generators of quantum dynamical semigroups, Commun. Math. Phys. **48**, 119 (1976).
[4] V. Gorini, A. Kossakowski, and E. C. G. Sudarshan, Completely positive dynamical semigroups of N-level systems, J. Math. Phys. (N.Y.) **17**, 821 (1976).
[5] H. P. Breuer and F. Petruccione, *The Theory of Open Quantum Systems* (Oxford University Press, New York, 2007), https://doi.org/10.1093/acprof:oso/9780199213900.001.0001.
[6] Christian Kraglund Andersen, Ants Remm, Stefania Lazar, Sebastian Krinner, Nathan Lacroix, Graham J. Norris, Mihai Gabureac, Christopher Eichler, and Andreas Wallraff, Repeated quantum error detection in a surface code, Nat. Phys. **16**, 875 (2020).
[7] Zaki Leghtas, Gerhard Kirchmair, Brian Vlastakis, Robert J. Schoelkopf, Michel H. Devoret, and Mazyar Mirrahimi, Hardware-efficient autonomous quantum memory protection, Phys. Rev. Lett. **111**, 120501 (2013).
[8] S. Touzard, A. Grimm, Z. Leghtas, S. O. Mundhada, P. Reinhold, C. Axline, M. Reagor, K. Chou, J. Blumoff, K. M. Sliwa, S. Shankar, L. Frunzio, R. J. Schoelkopf, M. Mirrahimi, and M. H. Devoret, Coherent oscillations inside a quantum manifold stabilized by dissipation, Phys. Rev. X **8**, 021005 (2018).
[9] K. W. Murch, U. Vool, D. Zhou, S. J. Weber, S. M. Girvin, and I. Siddiqi, Cavity-assisted quantum bath engineering, Phys. Rev. Lett. **109**, 183602 (2012).
[10] P. Magnard, P. Kurpiers, B. Royer, T. Walter, J.-C. Besse, S. Gasparinetti, M. Pechal, J. Heinsoo, S. Storz, A. Blais, and A. Wallraff, Fast and unconditional all-microwave reset of a superconducting qubit, Phys. Rev. Lett. **121**, 060502 (2018).
[11] E. T. Holland, B. Vlastakis, R. W. Heeres, M. J. Reagor, U. Vool, Z. Leghtas, L. Frunzio, G. Kirchmair, M. H. Devoret, M. Mirrahimi, and R. J. Schoelkopf, Single-photon-resolved cross-kerr interaction for autonomous stabilization of photon-number states, Phys. Rev. Lett. **115**, 180501 (2015).
[12] M. E. Kimchi-Schwartz, L. Martin, E. Flurin, C. Aron, M. Kulkarni, H. E. Tureci, and I. Siddiqi, Stabilizing entanglement via symmetry-selective bath engineering in superconducting qubits, Phys. Rev. Lett. **116**, 240503 (2016).
[13] Patrick M. Harrington, Erich J. Mueller, and Kater W. Murch, Engineered dissipation for quantum information science, Nat. Rev. Phys. **4**, 660 (2022).
[14] S. Nakajima, On quantum theory of transport phenomena: Steady diffusion, Prog. Theor. Phys. **20**, 948 (1958).
[15] R. Zwanzig, Ensemble method in the theory of irreversibility, J. Chem. Phys. **33**, 1338 (1960).
[16] Dorit Aharonov, Alexei Kitaev, and John Preskill, Fault-tolerant quantum computation with long-range correlated noise, Phys. Rev. Lett. **96**, 050504 (2006).

[17] Robert Alicki, Daniel A. Lidar, and Paolo Zanardi, Internal consistency of fault-tolerant quantum error correction in light of rigorous derivations of the quantum Markovian limit, Phys. Rev. A **73**, 052311 (2006).
[18] Mirko Rossini, Dominik Maile, Joachim Ankerhold, and Brecht I. C. Donvil, Single-qubit error mitigation by simulating non-Markovian dynamics, Phys. Rev. Lett. **131**, 110603 (2023).
[19] Daniel M. Reich, Nadav Katz, and Christiane P. Koch, Exploiting non-Markovianity for quantum control, Sci. Rep. **5**, 12430 (2015).
[20] Zhao-Di Liu, Yong-Nan Sun, Bi-Heng Liu, Chuan-Feng Li, Guang-Can Guo, Sina Hamedani Raja, Henri Lyyra, and Jyrki Piilo, Experimental realization of high-fidelity teleportation via a non-Markovian open quantum system, Phys. Rev. A **102**, 062208 (2020).
[21] Evangelos Vlachos, Haimeng Zhang, Vivek Maurya, Jeffrey Marshall, Tameem Albash, and E. M. Levenson-Falk, Master equation emulation and coherence preservation with classical control of a superconducting qubit, Phys. Rev. A **106**, 062620 (2022).
[22] M. M. Wolf, J. Eisert, T. S. Cubitt, and J. I. Cirac, Assessing non-Markovian quantum dynamics, Phys. Rev. Lett. **101**, 150402 (2008).
[23] Heinz-Peter Breuer, Elsi-Mari Laine, and Jyrki Piilo, Measure for the degree of non-Markovian behavior of quantum processes in open systems, Phys. Rev. Lett. **103**, 210401 (2009).
[24] Heinz-Peter Breuer, Elsi-Mari Laine, Jyrki Piilo, and Bassano Vacchini, Colloquium: Non-Markovian dynamics in open quantum systems, Rev. Mod. Phys. **88**, 021002 (2016).
[25] Ángel Rivas, Susana F. Huelga, and Martin B. Plenio, Entanglement and non-Markovianity of quantum evolutions, Phys. Rev. Lett. **105**, 050403 (2010).
[26] P. Haikka, J. D. Cresser, and S. Maniscalco, Comparing different non-Markovianity measures in a driven qubit system, Phys. Rev. A **83**, 012112 (2011).
[27] Yang Dong, Yu Zheng, Shen Li, Cong-Cong Li, Xiang-Dong Chen, Guang-Can Guo, and Fang-Wen Sun, Non-Markovianity-assisted high-fidelity Deutsch–Jozsa algorithm in diamond, npj Quantum Inf. **4**, 3 (2018).
[28] J. F. Haase, P. J. Vetter, T. Unden, A. Smirne, J. Rosskopf, B. Naydenov, A. Stacey, F. Jelezko, M. B. Plenio, and S. F. Huelga, Controllable non-Markovianity for a spin qubit in diamond, Phys. Rev. Lett. **121**, 060401 (2018).
[29] F. Wang, P.-Y. Hou, Y.-Y. Huang, W.-G. Zhang, X.-L. Ouyang, X. Wang, X.-Z. Huang, H.-L. Zhang, L. He, X.-Y. Chang, and L.-M. Duan, Observation of entanglement sudden death and rebirth by controlling a solid-state spin bath, Phys. Rev. B **98**, 064306 (2018).
[30] Ya-Nan Lu, Yu-Ran Zhang, Gang-Qin Liu, Franco Nori, Heng Fan, and Xin-Yu Pan, Observing information backflow from controllable non-Markovian multichannels in diamond, Phys. Rev. Lett. **124**, 210502 (2020).
[31] Jin-Shi Xu, Chuan-Feng Li, Ming Gong, Xu-Bo Zou, Cheng-Hao Shi, Geng Chen, and Guang-Can Guo, Experimental demonstration of photonic entanglement collapse and revival, Phys. Rev. Lett. **104**, 100502 (2010).
[32] Bi-Heng Liu, Li Li, Yun-Feng Huang, Chuan-Feng Li, Guang-Can Guo, Elsi-Mari Laine, Heinz-Peter Breuer, and Jyrki Piilo, Experimental control of the transition from Markovian to non-Markovian dynamics of open quantum systems, Nat. Phys. **7**, 931 (2011).
[33] Bi-Heng Liu, Dong-Yang Cao, Yun-Feng Huang, Chuan-Feng Li, Guang-Can Guo, Elsi-Mari Laine, Heinz-Peter Breuer, and Jyrki Piilo, Photonic realization of nonlocal memory effects and non-Markovian quantum probes, Sci. Rep. **3**, 1781 (2013).
[34] Nadja K. Bernardes, Alvaro Cuevas, Adeline Orieux, C. H. Monken, Paolo Mataloni, Fabio Sciarrino, and Marcelo F. Santos, Experimental observation of weak non-Markovianity, Sci. Rep. **5**, 17520 (2015).
[35] Kang-Da Wu, Zhibo Hou, Guo-Yong Xiang, Chuan-Feng Li, Guang-Can Guo, Daoyi Dong, and Franco Nori, Detecting non-Markovianity via quantified coherence: Theory and experiments, npj Quantum Inf. **6**, 55 (2020).
[36] Deepak Khurana, Bijay Kumar Agarwalla, and T. S. Mahesh, Experimental emulation of quantum non-Markovian dynamics and coherence protection in the presence of information backflow, Phys. Rev. A **99**, 022107 (2019).
[37] Xin-Yu Chen, Na-Na Zhang, Wan-Ting He, Xiang-Yu Kong, Ming-Jie Tao, Fu-Guo Deng, Qing Ai, and Gui-Lu Long, Global correlation and local information flows in controllable non-Markovian open quantum dynamics, npj Quantum Inf. **8**, 22 (2022).
[38] M. Gessner, M. Ramm, T. Pruttivarasin, A. Buchleitner, H-P. Breuer, and H. Häffner, Local detection of quantum correlations with a single trapped ion, Nat. Phys. **10**, 105 (2014).
[39] G. A. L. White, C. D. Hill, F. A. Pollock, L. C. L. Hollenberg, and K. Modi, Demonstration of non-Markovian process characterisation and control on a quantum processor, Nat. Commun. **11**, 6301 (2020).
[40] William K. Wootters, Entanglement of formation of an arbitrary state of two qubits, Phys. Rev. Lett. **80**, 2245 (1998).
[41] Shengshi Pang, Todd A. Brun, and Andrew N. Jordan, Abrupt transitions between Markovian and non-Markovian dynamics in open quantum systems, arXiv:1712.10109.
[42] See Supplemental Material at http://link.aps.org/supplemental/10.1103/PhysRevLett.132.200401 for further details on the experimental setup, system's Hamiltonian, numerical simulations, calibration of the parametric drive, device design, and quantum state tomography. The Supplemental Material contains additional references: [43–50].
[43] J. R. Johansson, P. D. Nation, and Franco Nori, QuTiP: An open-source PYTHON framework for the dynamics of open quantum systems, Comput. Phys. Commun. **183**, 1760 (2012).
[44] J. R. Johansson, P. D. Nation, and Franco Nori, QuTiP2: A PYTHON framework for the dynamics of open quantum systems, Comput. Phys. Commun. **184**, 1234 (2013).
[45] Arpit Ranadive, Martina Esposito, Luca Planat, Edgar Bonet, Cécile Naud, Olivier Buisson, Wiebke Guichard, and Nicolas Roch, Kerr reversal in Josephson meta-material and traveling wave parametric amplification, Nat. Commun. **13**, 1737 (2022).

[46] Priti Ashvin Shah *et al.*, qiskit-community/qiskit-metal: Qiskit Metal 0.1.5a1 (2023), https://doi.org/10.5281/zenodo.4618153.

[47] R. Barends, J. Kelly, A. Megrant, D. Sank, E. Jeffrey, Y. Chen, Y. Yin, B. Chiaro, J. Mutus, C. Neill, P. O'Malley, P. Roushan, J. Wenner, T. C. White, A. N. Cleland, and John M. Martinis, Coherent Josephson qubit suitable for scalable quantum integrated circuits, Phys. Rev. Lett. **111**, 080502 (2013).

[48] Zlatko K. Minev, Zaki Leghtas, Philip Reinhold, Shantanu O. Mundhada, Asaf Diringer, Daniel Cohen Hillel, Dennis Zi-Ren Wang, Marco Facchini, Priti Ashvin Shah, and Michel Devoret, pyEPR: The energy-participation-ratio (EPR) open- source framework for quantum device design (2021). https://github.com/zlatko-minev/pyEPR, https://pyepr-docs.readthedocs.io/en/latest/, https://doi.org/10.5281/zenodo.4744447.

[49] D. S. Wisbey, A. Martin, A. Reinisch, and J. Gao, New method for determining the quality factor and resonance frequency of superconducting micro-resonators from Sonnet simulations, J. Low Temp. Phys. **176**, 538 (2014).

[50] Pauli Virtanen *et al.* (SciPy 1.0 Contributors), SciPy1.0: Fundamental algorithms for scientific computing in Python, Nat. Methods **17**, 261 (2020).

[51] Jens Koch, Terri M. Yu, Jay Gambetta, A. A. Houck, D. I. Schuster, J. Majer, Alexandre Blais, M. H. Devoret, S. M. Girvin, and R. J. Schoelkopf, Charge-insensitive qubit design derived from the Cooper pair box, Phys. Rev. A **76**, 042319 (2007).

[52] Matthew Reagor *et al.*, Demonstration of universal parametric entangling gates on a multi-qubit lattice, Sci. Adv. **4**, eaao3603 (2018).

[53] S. A. Caldwell *et al.*, Parametrically activated entangling gates using Transmon qubits, Phys. Rev. Appl. **10**, 034050 (2018).

[54] Suman Kundu, Nicolas Gheeraert, Sumeru Hazra, Tanay Roy, Kishor V. Salunkhe, Meghan P. Patankar, and R. Vijay, Multiplexed readout of four qubits in 3D circuit QED architecture using a broadband Josephson parametric amplifier, Appl. Phys. Lett. **114**, 172601 (2019).

[55] Daniel F. V. James, Paul G. Kwiat, William J. Munro, and Andrew G. White, Measurement of qubits, Phys. Rev. A **64**, 052312 (2001).

[56] Valerie Coffman, Joydip Kundu, and William K. Wootters, Distributed entanglement, Phys. Rev. A **61**, 052306 (2000).

[57] M. Hatridge, S. Shankar, M. Mirrahimi, F. Schackert, K. Geerlings, T. Brecht, K. M. Sliwa, B. Abdo, L. Frunzio, S. M. Girvin, R. J. Schoelkopf, and M. H. Devoret, Quantum back-action of an individual variable-strength measurement, Science **339**, 178 (2013).

[58] P. M. Harrington, J. T. Monroe, and K. W. Murch, Quantum Zeno effects from measurement controlled qubit-bath interactions, Phys. Rev. Lett. **118**, 240401 (2017).

[59] B. Misra and E. C. G. Sudarshan, The Zeno's paradox in quantum theory, J. Math. Phys. (N.Y.) **18**, 756 (1977).

[60] Wayne M. Itano, D. J. Heinzen, J. J. Bollinger, and D. J. Wineland, Quantum Zeno effect, Phys. Rev. A **41**, 2295 (1990).

[61] K. Kakuyanagi, T. Baba, Y. Matsuzaki, H. Nakano, S. Saito, and K. Semba, Observation of quantum Zeno effect in a superconducting flux qubit, New J. Phys. **17**, 063035 (2015).

[62] S. Hacohen-Gourgy, L. P. García-Pintos, L. S. Martin, J. Dressel, and I. Siddiqi, Incoherent qubit control using the quantum Zeno effect, Phys. Rev. Lett. **120**, 020505 (2018).

[63] E. Blumenthal, C. Mor, A. A. Diringer, L. S. Martin, P. Lewalle, D. Burgarth, K. B. Whaley, and S. Hacohen-Gourgy, Demonstration of universal control between non-interacting qubits using the quantum Zeno effect, npj Quantum Inf. **8**, 88 (2022).

[64] D. H. Slichter, C. Müller, R. Vijay, S. J. Weber, A. Blais, and I. Siddiqi, Quantum Zeno effect in the strong measurement regime of circuit quantum electrodynamics, New J. Phys. **18**, 053031 (2016).

[65] Sabrina Patsch, Sabrina Maniscalco, and Christiane P. Koch, Simulation of open-quantum-system dynamics using the quantum Zeno effect, Phys. Rev. Res. **2**, 023133 (2020).

[66] Jay Gambetta, Alexandre Blais, M. Boissonneault, A. A. Houck, D. I. Schuster, and S. M. Girvin, Quantum trajectory approach to circuit QED: Quantum jumps and the Zeno effect, Phys. Rev. A **77**, 012112 (2008).

[67] Eissa Al-Nasrallah, Saurya Das, Fabrizio Illuminati, Luciano Petruzziello, and Elias C. Vagenas, Discriminating quantum gravity models by gravitational decoherence, Nucl. Phys. **B992**, 116246 (2023).